Design of Specific Peptide Inhibitors for Group I Phospholipase A_2: Structure of a Complex Formed between Phospholipase A_2 from *Naja naja sagittifera* (Group I) and a Designed Peptide Inhibitor Val-Ala-Phe-Arg-Ser (VAFRS) at 1.9 Å Resolution Reveals Unique Features[†,‡]

Rajendra Kumar Singh, P. Vikram, Jyoti Makker, Talat Jabeen, Sujata Sharma, Sharmistha Dey, Punit Kaur, A. Srinivasan, and Tej. P. Singh*

Department of Biophysics, All India Institute of Medical Sciences, New Delhi-110029, India

Received June 23, 2003; Revised Manuscript Received August 14, 2003

ABSTRACT: Phospholipase A_2 (PLA_2) (E. C. 3.1.1.4) is a common enzyme in the two-way cascade mechanism leading to the production of proinflammatory compounds known as eicosanoids. The binding of phospholipase A_2 to the membrane surface and hydrolysis of phospholipids are thought to involve the formation of a hydrophobic channel into which a single substrate molecule diffuses before its cleavage. To regulate the production of proinflammatory compounds, a specific peptide inhibitor Val-Ala-Phe-Arg-Ser (VAFRS) for the group I PLA_2 enzymes has been designed and synthesized. PLA_2 was isolated from Indian cobra (*Naja naja sagittifera*) venom and purified to homogeneity. The binding studies indicated the K_i value of $1.02 \pm 0.10 \times 10^{-8}$ M. The purified PLA_2 samples and the designed inhibitor VAFRS were cocrystallized. The crystal structure of the complex was determined and refined to 1.9 Å resolution. The peptide binds to PLA_2 at the active site and fills the hydrophobic channel completely. However, its placement with respect to the channel is in the opposite direction as compared to those observed in group II PLA_2's. Furthermore, the predominant intermolecular interactions involve strong electrostatic interactions between the side chains of peptide Arg and Asp 49 of PLA_2 together with a number of van der Waals interactions with other residues. A good number of observed interactions between the peptide and the protein indicate the significance of a structure-based drug design approach. The novel factor in the present sequence of the peptide is related to the introduction of a positively charged residue at the C-terminal part of the peptide.

Phospholipases A_2 (PLA_2: E. C. 3.1.1.4)[1] are involved in the catalysis of membrane phospholipids. In particular, they hydrolyze the sn-2 acyl bond of phospholipids producing equimolar amounts of lysophospholipids and free fatty acids. The ability of PLA_2 to produce substrates for the generation of inflammatory lipid mediators in the process of tissue injury and rheumatoid arthritis (*1*) makes this specific class of phospholipases as very important targets for the design of specific drugs against inflammation. The catalytic binding region in PLA_2's contains a comma-shaped hydrophobic channel with its head buried deep inside the molecule. The wall at the back of the channel contains key catalytic residues such as His 48 and Asp 49 behind which a disulfide link involving Cys51-Cys93 stabilizes the structure of the channel. Previously, we had focused on the design of inhibitors for group II PLA_2's with an aromatic head containing an OH group on one side and linking a hydrocarbon chain on the other side. Using the above approach, the complexes of PLA_2 with two natural inhibitors aristolochic acid (*2*) and α-tocopherol (*3*) were examined. The structure of a complex formed between PLA_2 and a native peptide FLSYK that showed significantly higher inhibition rate than the two natural compounds mentioned above having OH groups and a basic side chain was also analyzed (*4*). The structure of yet another complex of PLA_2 formed with a designed peptide LAIYS that contained residues with OH groups and hydrophobic side chains was also analyzed in detail (*5*). On the basis of the above, a number of peptides with various combinations involving residues with OH groups such as Tyr and Ser, with basic side chains such as Arg and Lys and hydrophobic residues such as Ala, Val, Leu, Ile, and Phe were synthesized. Several newly designed peptides showed significant inhibitions against various group II PLA_2 (*6*). To further examine the potency of rationally designed peptides against group I PLA_2's, the complex of PLA_2 was formed with a peptide Val-Ala-Phe-Arg-Ser (VAFRS) and its detailed crystal structure is reported here. Since the PLA_2

[†] The author acknowledges the financial assistance from Department of Biotechnology, Government of India, New Delhi. Rajendra Kumar Singh, Jyoti Makker, and Talat Jabeen thank the Council of Scientific and Industrial Research, New Delhi for the award of fellowships.

[‡] The atomic coordinates have been deposited in the protein data bank with entry 1MF4.

* To whom correspondence should be addressed: T. P. Singh, Department of Biophysics, All India Institute of Medical Sciences, Ansari Nagar, New Delhi − 110 029, India, Tel: +91-11-2658 8931. FAX: +91-11-2658 8663. E-mail: tps@aiims.aiims.ac.in.

[1] Abbreviations: DMF, dimethyl formamide; HBTU, 2-(1H-benzotriazole-1-yl)-1,1,3,3-tetramethyl uronium hexa fluorophosphates; NMM, *N*-methyl morpholine; PLA_2, phospholipase A_2; PDB, protein data bank; rms, root-mean-squares; SDS−PAGE, sodium dodecyl sulfate−polyacrylamide gel electrophoresis; TFA, trifluoroacetic acid.

10.1021/bi035076x CCC: $25.00
Published on Web 09/19/2003

used in the present studies is from a snake venom, it can be termed as a surrogate PLA_2 enzyme.

EXPERIMENTAL PROCEDURES

Purification of PLA_2. The crude venom of south Indian/Andaman sub-species *Naja naja sagittifera* was obtained from the Irula snake farm in Tamilnadu (India). A total of 250 mg of venom was dissolved in 25 mL of deionized water. The solution was centrifuged at 16 000 rpm for 20 min to remove insoluble materials. The collected supernatant was diluted with the same amount of 50 mM ammonium acetate buffer pH 6.0 and was loaded on a preequilibrated column with the same buffer containing Cibacron Blue CL-6B (Pharmacia). The column was washed with 20 mM ammonium acetate buffer, pH 6.0 to remove unbound fractions. In the next step, 50 mM ammonium bicarbonate buffer pH 8.0 was passed through the column to remove weakly bound proteins. Finally, 20 mM ammonium carbonate buffer pH 10.5 was used to elute the bound PLA_2. The bound fractions were dialyzed against ammonium acetate buffer, pH 7.5. Then, it was loaded on a DEAE-Sephacel anion exchanger column at the same pH. To elute the acidic PLA_2, a salt gradient of NaCl (0.0−0.5 M) in 50 mM ammonium acetate buffer, pH 7.5 was used; the fractions having PLA_2 activity were eluted at 0.25 M NaCl. These fractions were dialyzed against ammonium acetate buffer, pH 7.5. To remove other minor contaminants, it was further passed through a SP-Sephadex cation exchanger column equilibrated with the ammonium acetate buffer, pH 7.5. The unbound fractions were collected and dialyzed against water to remove salt. The samples were lyophilized and their purity was checked with sodium dodecyl sulfate−polyacrylamide gel electrophoresis (SDS−PAGE), by determining the N-terminal sequence and by activity measurements.

Synthesis of Peptide VAFRS. The peptide was synthesized using an automated solid-phase peptide synthesizer (Rainin, USA). The resin used was Fmoc-Ser-Wang resin, and the solvent used for synthesis was dimethyl formamide (DMF). In the first step, Fmoc-Ser-Wang resin (1 g, 0.5 mM) was deprotected by 20% piperadine in DMF to form H_2N-Ser-Wang resin. The uronium salt 2-(1H-benzotriazole-1- yl)-1,1,3,3-tetramethyl uronium hexa fluorophosphates (HBTU) (455 mg, 1 mM) in the presence of base *N*-methyl morpholine (NMM; 0.4 M) activated the amino acid to form the acetic ester of Fmoc-Arg-OH (551 mg, 0.5 mM). This was coupled with H_2N-Ser-Wang resin to get Fmoc-Arg-Ser-Wang resin. The above procedure was repeated for the remaining amino acids until the complete sequence Fmoc-Val-Ala-Phe-Arg-Ser-Wang resin was formed. The resin was cleaved from the peptide with trifluoroacetic acid (TFA). The peptide was purified using reverse phase chromatography on C_{18} Rep RPC column (1.6 × 1.0 cm, Pharmacia, Hong Kong). The purity of the peptide was confirmed with MALDI-TOF (Kratos, Shimadzu) and also by determining its amino acid sequence with a PPSQ-21A protein sequencer (Shimadzu, Japan).

Kinetic and Inhibition Studies of PLA_2 with VAFRS. The purified samples of PLA_2 were used in the kinetic studies. All assays were carried out using phosphatidylcholine as substrate (Sigma). Assays were performed in 20 mM glycyl-glycine buffer (pH 7.5) containing 3 mM $CaCl_2$ at 25 °C using 0.05 M cresol red as indicator. The enzyme concentration was fixed at 1.5 μM. The enzyme was incubated with 5×10^{-9}−10^{-7} M of VAFRS under the above-mentioned conditions for 1 h. The amount of free enzyme was determined by the addition of 0.25−1 mM substrate. The volume of the substrate solution comprised 5% of the total reaction mixture. The initial velocity was calculated from the changes in absorbance at 578 nm recorded with Perkin-Elmer spectrophotometer (model-Lambda 25). The data were analyzed using the Lineweaver−Burk method (*7*).

Crystallization. Purified samples of PLA_2 were dissolved in 10 mM sodium phosphate buffer, pH 6.0 containing 1 mM $CaCl_2$ to a final protein concentration of 2.5 mg/mL. The peptide VAFRS was added to the protein solution at 10 times higher molar concentration. This was mixed well and 15 μL drops of the above mixture were equilibrated in a hanging drop vapor diffusion method against the same buffer containing 35% ethanol in the reservoir. The regular shaped colorless crystals of dimensions up to 0.3 × 0.2 × 0.2 mm were obtained at 298 K after about three weeks.

Data Collection. The crystals of the complex formed between PLA_2 and peptide VAFRS were stable in the X-ray beam for more than 24 h. One crystal with dimensions (0.3 × 0.2 × 0.2) mm was used for intensity data collection. The X-ray intensity data were collected at 278 K with a MAR research, 300-mm diameter imaging plate scanner mounted on a RU-200 rotating anode X-ray generator equipped with a graphite monochromator. The intensities were integrated using DENZO and SCALEPACK programs (*8*). The crystals belong to space group $P4_1$ with unit cell parameters $a = b = 42.8$ Å, $c = 65.9$ Å containing four molecules in the unit cell. The data have an overall R_{sym} of 7.3% with an overall completeness of 92% to 1.9 Å resolution. The statistics of crystallographic data are listed in Table 1.

Structure Determination and Refinement. As this is a new isoform of PLA_2 from a different species of cobra, the structure was determined by the molecular replacement method with AmoRe (*9*) using the model of PLA_2 from *Naja naja naja* (PDB code: 1PSH). After rigid body refinement, it yielded an R-factor of 42.3% and a correlation coefficient of 56.7%. The solution was transformed from Eulerian coordinates to orthogonal coordinates. These coordinates were used for refinement.

The refinement was carried out with the program REFMAC 4.01 (*10*). In each step, $2F_o-F_c$ and F_o-F_c maps were calculated to improve the structure with the help of electron density maps using the program O (*11*). The individual B factors were refined. The positions of 105 water molecules were located from difference Fourier maps using a cut off of 2.5σ. Both Fourier and difference Fourier maps computed at this stage clearly indicated the presence of the peptide VAFRS at the binding site of the protein molecule. However, the electron density for serine of the peptide was absent. In the subsequent steps of refinement, the coordinates of the peptide molecule were also included. Even at the end of refinement, the density for serine in the peptide did not improve, indicating that it may not be involved in the intermolecular interactions and may be wagging freely on the surface of protein molecule. The details of the refinement and other parameters are listed in Table 1.

Table 1: Data Collection and Refinement Statistics

space group	$P4_1$
unit cell dimensions (Å)	
$a = b$	42.8
c	65.9
no. of reflections collected	8668
no. of unique reflections	8247
resolution range (Å)	20.0−1.9
overall completeness (%)	92.0
completeness in the highest resolution shell (1.97−1.90)%	61.3
overall R_{sym} (%)	7.3
R_{sym} in the highest resolution shell (1.97−1.90)	(%15.6)
overall I/σ	9.3
I/σ in the highest resolution shell (1.97−1.90)	2.1
V_m (Å^3/Da)	2.26
solvent content (%)	45.1
Z	4
PDB entry for the present structure	1MF4
PDB entry for the native PLA_2 structure	1LFF
R factor (%)	18.2
free- R factor (%)	23.9
protein atoms	909
peptide inhibitor (VAFRS) atoms	41
calcium ion	1
water molecules	105
rms deviations from ideal values in	
bond lengths (Å)	0.011
bond angles (deg)	1.7
torsion angles (°)	17.0
average B factors (Å^2)	
from Wilson Plot	20.6
for main chain atoms	22.6
for side chain atoms and solvent atoms	28.1
for inhibitor atoms	53.5
for Ca^{2+} ions	24.3
for all atoms	25.5
residues in the most allowed regions (%)	88.8
residues in the additionally allowed regions (%)	11.2

RESULTS AND DISUSSION

Quality of the Model. The final model consists of 908 protein atoms, 41 peptide inhibitors atoms, 1 phosphate ion, and 105 water molecules. The dispersion precision indicator (*12*, *13*) estimates an average root-mean-square (rms) coordinate error of 0.14 Å. The conformational space as defined by the program PROCHECK (*14*) indicate that the 88.8% of the nonglycine and non-Pro residues fall in the most favored regions of the Ramachandran plot (*15*). The remaining 11.2% residues were found in the additionally allowed regions. The ϕ, φ torsion angles for the peptide molecule indicate that all the peptide residues belong to the additionally allowed regions of the map.

Inhibition of PLA_2 by the Peptide VAFRS. The purified samples of $CPLA_2$ were used for inhibition studies. It may be mentioned here that the PLA_2's show a higher activity with aggregated substrates such as natural membranes (*16*). This is known as interfacial catalysis, which includes binding of the enzyme at the lipid−aqueous interface and activation steps (*17*). In the present case, the substrate concentrations were kept above the critical micellar concentration. As a result, it was present as an aggregated system. Although it might not have been an identical condition to that of the native substrate, it could be considered as a fairly similar environment. The PLA_2 activity was inhibited by the peptide in a dose-dependent manner. The calculated IC_{50} value was $2.35 \pm 0.06 \times 10^{-8}$ M. The kinetic experiments indicated that the peptide acted as a competitive inhibitor of $CPLA_2$

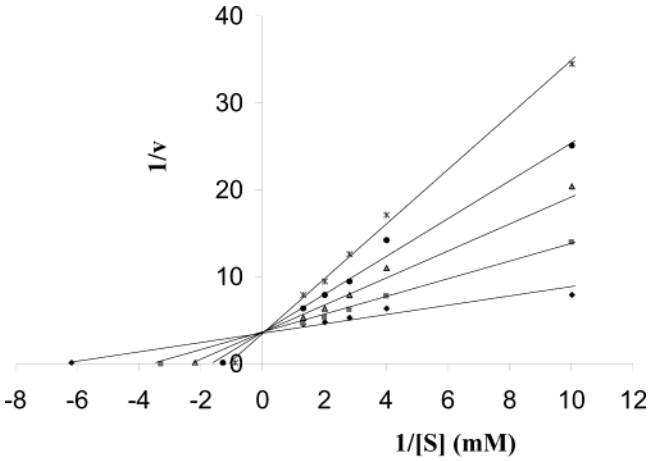

FIGURE 1: Lineweaver-Burk plot of inhibition of PLA_2 by VAFRS. The assays were carried out at 25 °C in 20 mM glycylglycine buffer (pH 7.5) containing 3 mM $CaCl_2$ using 0.05 M cresol red as indicator. The enzyme concentration was 1.5 μM. The peptide concentrations were 5×10^{-9} M (■), 1×10^{-8} M (▲), 5×10^{-8} M (●), 1×10^{-7} M (×), and control (♦).

Table 2: Binding Constants of Peptides, VAFRS, FLSYK, and LAIYS with Group I ($CPLA_2$) and Group II ($DPLA_2$)

	group I ($CPLA_2$)	group II ($DPLA_2$)
VAFRS	$1.02 + 0.02 \times 10^{-8}$ M	$5.37 \pm 0.06 \times 10^{-7}$ M
FLSYK	$8.56 \pm 0.07 \times 10^{-7}$ M	$3.57 \pm 0.05 \times 10^{-9}$ M
LAIYS	$2.64 \pm 0.04 \times 10^{-7}$ M	$3.74 \pm 0.08 \times 10^{-8}$ M

and the estimated K_i value was $1.02 \pm 0.10 \times 10^{-8}$ M (Figure 1). The calculated K_M value for the substrate was found to be $1.65 \pm 0.02 \times 10^{-4}$ M. The binding constants for VAFRS, FLSYK, and LAIYS with type I $CPLA_2$ and type II $DPLA_2$ obtained under identical conditions are listed in Table 2.

Binding of VAFRS. Excellent electron density for VAFRS was observed at the binding site of $CPLA_2$ (Figure 2a) which allowed a detailed description of the interactions between $CPLA_2$ and the peptide VAFRS. The peptide atoms had a moderate B value of 53.5 Å^2. All the peptide residues were found in the additionally allowed regions of the map. The peptide molecule covered an extensive surface area of 915.2 Å^2 in the enzyme (Figure 2b). All these suggested a high compatibility of the peptide structure with the binding site in the enzyme. As the inhibitor molecule diffuses into the hydrophobic channel, it is expected to interact with its constituents, including the residues of the active site. As seen from Table 3, the binding of peptide is stabilized by electrostatic interactions involving Arg of the peptide and Asp 49, and a number of hydrogen bonds formed between the inhibitor and the enzyme. It also forms a number of hydrophobic interactions with the residues of the hydrophobic channel (data not shown). Hereafter, peptide atoms will be indicated with a letter P in parentheses to distinguish them from protein residues. As stated above, the most striking interactions are observed involving the side chain of Arg (P) which interacts with Asp 49 electrostatically and forms a number of other hydrogen bonds with His 48, Cys 45, Tyr 28, and water molecule OW 88 (Figure 3). It also forms a large number of hydrophobic interactions with Lys 31, Tyr 64, Ala 23, Phe 22, Trp 19, Ile 9, and Lys 6, thus completely filling the binding site of $CPLA_2$ (Figure 2b). Although Ser-(P) is involved in a number of hydrophic interactions with

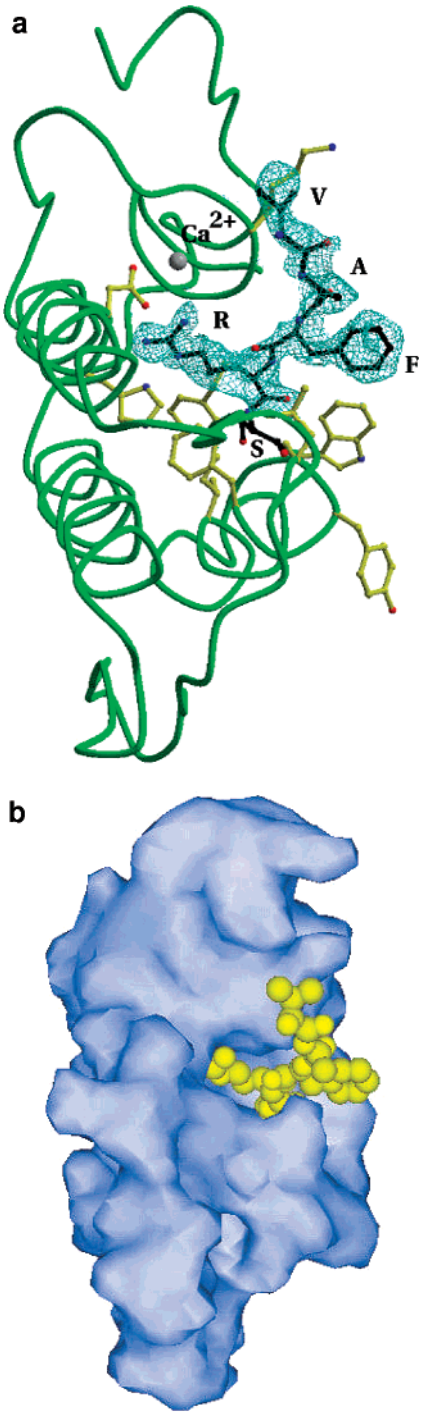

FIGURE 2: (a) The F_o-F_c map contoured at 2σ showing the electron density for the peptide Val-Ala-Phe-Arg-Ser. Some of the protein residues of the hydrophobic channel are indicated in yellow. (b) Grasp (*18*) representation of the binding cavity and the hydrophobic channel. The peptide VAFRS is almost completely buried in the pocket.

protein residues on the surface, its position, as reflected by the poor electron density is not well defined. It may be attributed to the nonspecific nature of van der Waals interactions involving Ser(P). The binding studies of VAFRS and VAFR with PLA_2 indicated a higher affinity for VAFRS as compared to VAFR (data not shown), suggesting an advantage of extending VAFR to VAFRS. Some of the interactions in the present complex are distinct from those observed in the complexes of peptide inhibitors FLSYK (*4*)

Table 3: Hydrogen Bonded and Hydrophobic Interactions (<3.5 Å) between the Protein ($CPLA_2$) and the Designed Peptide (VAFRS)

peptide	protein	distance (Å)
Val 1 C^{β}	Lys 31 C^{γ}	3.4
	Lys 31 C^{ϵ}	3.3
Ala 2 N	Tyr 64 OH	3.2
Ala 2 C^{β}	Tyr 64 $C^{\epsilon 2}$	3.0
Arg 4 NE	His 48 $N^{\delta 1}$	3.5
Arg 4 NH1	Tyr 28 O	3.2
	Asp 49 $O^{\delta 1}$	2.7
	Wat 88	2.9
Arg 4 NH2	Cys 45 O	3.0
	His 48 $N^{\delta}1$	2.7
	Asp 49 $O^{\delta 1}$	2.4
Arg 4 C^{β}	Ala 23 C^{δ}	3.5
Ser 5 C^{α}	Ile 9 C^{α}	3.0
Ser 5 C^{β}	Ile 9 $C^{\delta}1$	3.0
	Phe 22 C^{β}	3.1
	Phe 22 $C^{\delta 2}$	3.4
	Trp 19 C^{α}	3.4
	Trp 19 C	3.2
Ser 5 O^{γ}	Trp 19 O	3.0
Ser 5 C	Trp 19 $C\beta$	3.0
	Trp 19 C^{γ}	3.5
	Trp 19 $C^{\delta 2}$	3.5
	Trp 19 $C^{\epsilon 2}$	3.0
	Lys 6 C^{γ}	3.3

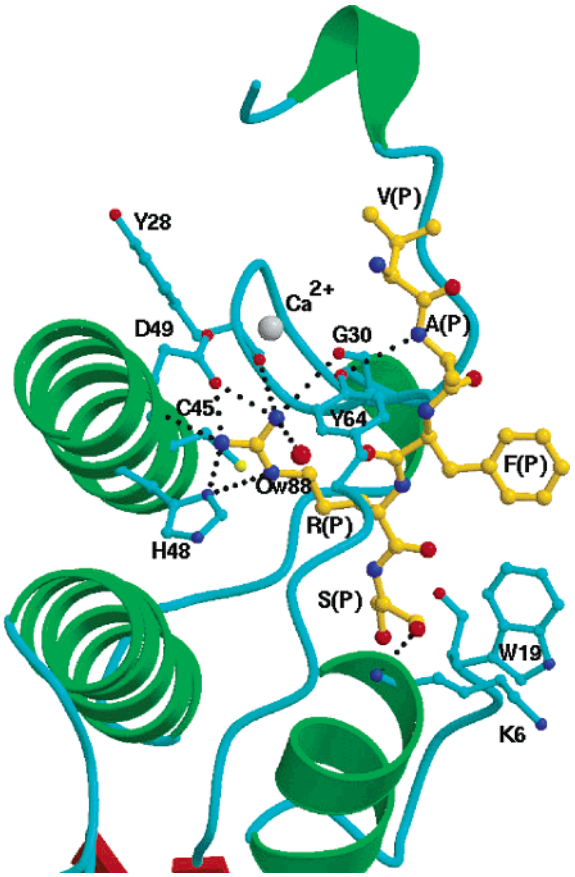

FIGURE 3: Interactions between PLA2 and the peptide Val-Ala-Phe-Arg-Ser. The peptide residues are indicated with a P in parentheses. The critical interactions between Arg(P) side chain and His 48 $N^{\delta 1}$ and Asp 49 $O^{\delta 1}$ including other hydrogen bonds between peptide and protein are shown by a dotted line.

and LAIYS (*5*) with a group II PLA_2 enzyme (*Daboia Russelli Pulchella*, $DPLA_2$) (*19*). The main difference between the shapes of the hydrophobic channels formed in group I (present structure of $CPLA_2$) and group II ($DPLA_2$,

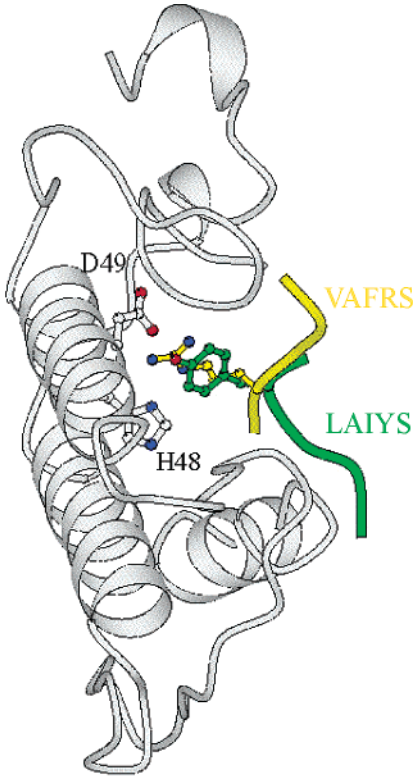

FIGURE 4: The placement of inhibitor peptides in PLA_2's of groups I (VAFRS: yellow) and II (LAIYS: green). The target residues of protein His 48 and Asp 49 interact with Arg (VAFRS) and Tyr (LAIYS) side chains while the main chains of peptides are aligned in opposite directions.

18) is in the direction of the opening to the hydrophobic channel. The Trp 19 in $CPLA_2$ and Trp 31 in $DPLA_2$ function as the regulatory flaps in the two structures. In $CPLA_2$, Trp 19 is located at the lower wall of the channel and rearranges upon its binding, while in $DPLA_2$, Trp31 is situated at the upper wall and moves downwardly upon interactions with the bound inhibitors (*5*). As a result of the these unique features in two types of PLA_2's, the overall shapes of the hydrophobic channels with respect to the active site residues and the placement of peptide inhibitors in the two types of structures differ remarkably (Figure 4). The interactions of the inhibitors at the interior of the channel in the complexes of types I and II PLA_2's are similar, while those on the surface differ considerably (Table 4**).** Thus, the above features of the hydrophobic channels in types I and II PLA_2's are important to be kept in mind while designing their specific inhibitors.

Comparison of the Structures of $CPLA_2$ in the Present Complex with that in the Native State. The overall structures of $CPLA_2$ in the native (1LFF) and complexed states are essentially similar with the root-mean-squares (rms) shift of 0.3 Å in their C^α positions as the binding of peptide VAFRS does not perturb the structure of the enzyme significantly. The orientation of Trp 19 in the structure of the complex when compared with its orientation in the native structure is only slightly changed. The calcium binding loop that constitutes one of walls of the hydrophobic channel also shows only a small shift from the corresponding loop in the native structure (rms shift for C^α atoms for residues 27−34 is 0.6 Å). Accordingly, the position of Ca^{2+} ion is shifted by 0.7 Å. This shows that the peptide molecule fits well in the binding site of the enzyme without significantly perturbing the structure of the enzyme.

Table 4: Hydrogen Bonded Interactions between Interacting Protein and Inhibitor Atoms

	designed peptide inhibitors					
protein	$CPLA_2$ VAFRS		$DPLA_2$ LAIYS		$DPLA_2$ FLSYK	
Leu 3 N			Leu 1 O	3.2		
Leu 3 O					Phe 1 N	2.6
Gly 6 N			Ala 2 O	2.8	Ser 3 N	3.3
Lys 7 N					Phe 1 N	2.7
Trp/Ile 19 N	Ser 5 O^γ	3.1			Leu 2 O	2.8
Tyr 28 O	Arg 4 NH1	3.2			Lys 5 N^ζ	3.2
Gly 30 O					Lys 5 N	3.3
					Lys 5 N^ζ	3.0
Trp 31 $N^{\epsilon 1}$			Ser 5 O^γ	2.6		
Gly 32 O					Lys 5 N^ζ	2.6
Cys 45 O	Arg 4 NH2	3.0				
His 48 $N^{\delta 1}$	Arg 4 NH2	2.7	Tyr 4 OH	3.0	Lys 5 O	2.9
	Arg 4 NE	3.5				
Asp 49 $O^{\delta 1}$	Arg 4 NH2	2.5	Tyr 4 OH	2.9	Lys 5 N^ζ	3.3
	Arg 4 NH1	2.7				
Asp 49 $O^{\delta 2}$					Lys 5 N^ζ	2.9
Tyr 64 OH	Ala 2 N	3.2				
Wat	Arg 4 NH1	2.9	Leu 1 N	3.1	Phe 1 O	3.3
	Phe 3 O	2.7	Leu 1 N	2.9	Tyr 4 OH	3.0
			Tyr 4 O	2.8		
			Tyr 4 OH	3.2		

CONCLUSIONS

The present structure clearly indicates that the best inhibitor for group I PLA_2's may not necessarily be the best inhibitor for group II PLA_2's as the channels in the structures of two types of PLA_2's are molded differently at the outer surface of the molecule. In group I PLA_2's, it turns upward while in group II, it binds downward. Therefore, the design should accordingly incorporate appropriate residues in the two parts of the peptide to take into account the stereochemical and aspects of the binding channel. The comparative binding studies with LAIYS, FLSYK, and VAFRS with $CPLA_2$ and $DPLA_2$ indeed highlight these interesting disparities when used against the two types of enzymes. Thus, to inhibit the PLA_2's of both groups simultaneously, it may be necessary to incorporate two independent molecules with specificities directed separately.

REFERENCES

1. Wery, J. P., Schevitz, R. W., Clawson, D. K., Bobbitt, J. L., Dow, E. R., Gamboa, G., Goodson, T., Jr., Hermann, R. B., Kramer, R. M., and McClure, D. B. (1991) *Nature 352*, 79−82.
2. Chandra, V., Jasti, J., Kaur, P., Srinivasan, A., Betzel, C., and Singh T. P. (2002) *Biochemistry 41*, 10914−10919.
3. Chandra, V., Jasti, J., Kaur, P., Betzel, C., Srinivasan, A., and Singh, T. P. (2002) *J. Mol. Biol. 320*, 215−222.
4. Chandra, V., Jasti, J., Kaur, P., Dey, S., Perbandt, M., Srinivasan, A., Betzel, C., and Singh, T. P. (2002) *J. Biol. Chem. 277*, 41079−41085.
5. Chandra, V., Jasti, J., Kaur, P., Dey, S., Srinivasan, A., Betzel, C., and Singh, T. P. (2002) *Acta Crystallogr. D58*, 1813−1819.
6. Makker, J. (2002) Ph. D. dissertation submitted to All India Institute of Medical Sciences.
7. Lineweaver, H., and Burk, D. (1934) the determination of enzyme dissociation constants. *J. Am. Chem. Soc. 56*, 658−666.

8. Otwinowski, Z., and Minor, W. (1997) *Methods Enzymol. 176*, 307−326.
9. Navaza, J., (1994) *Acta Crystallogr. A50*, 157−163.
10. Collaborative computational project number 4 (1994) The CCP4 suite: programs for protein crystallography. *Acta Crystallogr. D50*, 760−763.
11. Jones, T. A., Zou, J. Y., Cowan, S. W., and Kjeldgaard, M. (1991) *Acta Crystallogr. A47*, 110−119.
12. Cruickshank, D. W. J. (1999) *Acta Crysallogr. D55*, 583−601.
13. Murshudov, G. N., and Dodson, E. J. (1997) CCP4 Newslett. *Protein Crystallogr. 33*, 31−39.
14. Laskowski, R., Macarthur, M., Moss, D., and Thornton, J. (1993) *J. Appl. Crystallogr. 26*, 283−290.
15. Ramachandran, G. N., and Sasisekharan, V. (1968) *Adv. Protein Chem. 23*, 713−720.
16. Yaun, W., Quinn, D. W., Sigler, P. B., and Gelb, M. H. (1990) *Biochemistry 29*, 6082−6094.
17. Scot, D. L., White, S. P., Otwinoski, Z., Yuan, W., Gelb, M. H., and Sigler, P. B. (1990) *Science 250*, 1541−1546.
18. Nicholls, A., Sharp, K., and Honig, B. (1991) *Proteins 11*, 281−296.
19. Chandra, V., Kaur, P., Jasti, J., Betzel, C., and Singh, T. P. (2001) *Acta Crystallogr. D* 57, 1793−1808.

BI035076X